Chemico-Biological Interactions 285 (2018) 85–95

Contents lists available at ScienceDirect

Chemico-Biological Interactions

journal homepage: www.elsevier.com/locate/chembioint

miR-501 is upregulated in cervical cancer and promotes cell proliferation, migration and invasion by targeting CYLD

Jaceline Gislaine Pires Sanches[a], Yunchao Xu[a], Iddrisu Baba Yabasin[d], Min Li[a], Ying Lu[e], Xiaoxin Xiu[f], Lu Wang[a], Limin Mao[e], Jie Shen[e], Bo Wang[a], Li Hou[a], Jingfang Ju[c], Junjun Zhao[b,**], Bo Song[a,*]

[a] Department of Pathology and Forensics, Dalian Medical University, Dalian 116044, China
[b] Department of Pathology, Dalian Municipal Central Hospital, Dalian 116033, China
[c] Translational Research Laboratory, Department of Pathology, Stony Brook University, Stony Brook, NY 11794, USA
[d] Department of Anesthesia, First Affiliated Hospital of Dalian Medical University, Dalian 116011, China
[e] Teaching Laboratory of Morphology, Dalian Medical University, Dalian 116044, China
[f] Department of Gynecology and Obstetrics, First Affiliated Hospital of Dalian Medical University, Dalian 116011, China

ARTICLE INFO

Keywords:
miR-501
Cervical cancer
CYLD
Cell proliferation
Invasion

ABSTRACT

Background: Cervical cancer is the common gynecological deadly malignancy worldwide. Here we attempted to evaluate the effects and mechanisms of microRNA-501-5p (miR-501) on the cell proliferation, migration, invasion and the clinical significance in the cervical cancer.

Methods: Cervical cancer HeLa cells were transfected with miR-501 mimic or inhibitor or siRNA against Cylindromatosis (CYLD) using Lipofectamine 2000. miR-501 expression was assessed in HeLa cells and cervical cancer specimens by real-time qRT-PCR. The functional roles of miR-501 were determined by CCK-8, colony formation, scratch wound healing and transwell assays. The apoptosis rate was detected by flow cytometry assay. CYLD, BCL-2, BAX, NF-κB p65 and phosphorylated p65 (p-p65) proteins were examined by Western blotting. CYLD expression was evaluated by immunohistochemistry in cervical cancer tissues.

Results: miR-501 was upregulated, whereas CYLD protein was downregulated in cervical cancer tissues compared to normal cervical tissues. miR-501 overexpression and CYLD protein downregulation were positively correlated with poor differentiation, tumor size, International Federation of Gynecology and Obstetrics (FIGO) stage and lymph node metastasis. CYLD was downregulated by miR-501 at both mRNA and protein levels in HeLa cells. miR-501 promoted cell proliferation, migration and invasion in cervical cancer, while inhibited the apoptosis. This is possibly due to the downregulation of CYLD and subsequent activation of NF-κB p65.

Conclusions: miR-501 upregulation and CYLD downregulation are associated with the development and progression of cervical cancer. miR-501 promotes cervical cancer cell proliferation, migration and invasion possibly via downregulating CYLD and subsequently activating NF-κB p65. miR-501 might be a potential therapeutic target for cervical cancer.

1. Introduction

Cervical cancer is a common gynecological malignancy that has been reported to be a leading cause of cancer-related mortality among women worldwide [1–3]. Human papilloma virus (HPV) is believed to play a major role in the etiology of cervical cancer, though some other factors may also be involved [4]. Currently surgery, radiation and chemotherapy combination improve the prognosis of cervical cancer, however, a considerable number of patients at late stage still suffer from the metastasis and recurrence [5].

microRNAs (miRNAs) are a class of endogenous short noncoding RNAs that inhibit post-transcriptional gene expression by binding to

Abbreviations: miR-501, microRNA-501-5p; CYLD, Cylindromatosis; NC, negative Control; miR-501, miR-501 mimic; 501i, miR-501 inhibitor; siCYLD, siRNA against CYLD; CCK-8, Cell Counting Kit 8; FIGO, International Federation of Gynecology and Obstetrics; PBS, Phosphate buffer solution; SDS-PAGE, Sodium dodecyl sulfate-poly acrylamide gel electrophoresis; qRT-PCR, quantitative real time-polymerase chain reaction; FFPE, Formalin-fixed and paraffin-embedded; IHC, Immunohistochemistry; DAB, Diaminobenzidine; DPX, p-xylene-bis-pyridinium bromide; PI, Propedium iodide

* Corresponding author.
** Corresponding author.
E-mail addresses: jjsx528@126.com (J. Zhao), songbo9177@163.com (B. Song).

https://doi.org/10.1016/j.cbi.2018.02.024
Received 12 December 2017; Received in revised form 24 January 2018; Accepted 19 February 2018
Available online 23 February 2018
0009-2797/

target mRNA at their 3′-untranslated region (3′-UTR) [6]. They are key players in various critical cellular processes such as proliferation, cell cycle progression, apoptosis and differentiation [7–11]. During the past decade, miRNAs aberration has been found to be involved in the tumorigenesis and progression in various types of malignancies including cervical cancer [12–18]. miRNAs may be the optimal candidates as the biomarkers for diagnosis and prognosis, and may also be the potential therapeutic targets [19,20].

Recently discovered oncomir microRNA-501-5p (miR-501) is a non-conserved miRNA emerging as a potential key player in tumorigenesis. miR-501 was found to be overexpressed in hepatocellular carcinoma (HCC) HepG2 cells and tissues with high-hepatitis B virus (HBV) replication [21]. Huang et al. [22] also reported that miR-501 is upregulated in the HCC cells and tissues, and miR-501 enhances the proliferation of HCC cells in vitro through decreased Cylindromatosis (CYLD) and increased cyclin D1 and c-myc expressions. Recently Zhang et al. [23] screened the key miRNAs for HCC using miRNA-mRNA functional synergistic network and found that miR-501 is the most significantly upregulated miRNA in HCC tissues. Another study demonstrated that miR-501 is overexpressed in gastric cancer cell lines and human gastric cancer tissues, and high miR-501 expression could be a poor overall survival predictor in gastric cancer patients. In addition, miR-501 promotes gastric cancer stem cell like phenotype by directly targeting DKK1, NKD1 and GSK3β and subsequent activated Wnt/β-catenin signalling [24]. miR-501 is also reported to be upregulated in the conjunctival malignant melanoma and retinoblastoma [25,26]. However, the impacts and underlying mechanisms of miR-501 on the cervical cancer have not been explored.

CYLD was originally identified as a gene mutated in familial cylindromatosis (FC) which is described as a genetic disorder predisposing for the development of tumors of skin appendages, termed cylindroma [27]. CYLD gene is map on chromosome 16q12.1 and its C-terminal region contains a catalytic domain with sequence homology to ubiquitin-specific peptidases (USP) family members [27,28]. CYLD gene mutations are also associated with multiple familial trichoepithelioma (MFT) and multiple myeloma [29–31]. Additionally, comparative genomic hybridization (CGH) assay revealed reduced copy number of CYLD in kidney cancer, HCC and glassy cell carcinoma cell lines of the uterine cervix [32–34]. Meanwhile, suppressed CYLD gene expression was found in the colorectal cancer, breast cancer and lung cancer [35–37]. Thus, CYLD is considered as a tumor suppressor. Moreover, CYLD has been reported to bind to IKK gamma, a component of the IkappaB kinase (IKK) complex, and negatively regulate the nuclear factor-kappa B (NF-κB) activity [38].

In the present study, we investigated the roles of miR-501 on cervical cancer in vitro and its correlation with the clinicopathologic features. We found that CYLD was downregulated by miR-501 at both mRNA and protein levels in the cervical cancer HeLa cells. The in vitro experiments showed that miR-501 promoted cervical cancer cell proliferation, migration and invasion, while inhibited apoptosis. NF-κB p65, phosphorylated p65 (p-p65) and BCL-2 expressions were increased and BAX was decreased while CYLD was downregulated by miR-501. In addition, miR-501 was overexpressed and CYLD protein was reduced in the cervical squamous cancer tissues compared to the adjacent normal cervical squamous epithelium. Furthermore, miR-501 overexpression and CYLD downregulation were positively correlated with poor differentiation, tumor size, International Federation of Gynecology and Obstetrics (FIGO) stage and lymph node metastasis. Therefore, our results suggest that miR-501 promotes cervical cancer cell proliferation, migration and invasion possibly through downregulating CYLD and activating NF-κB p65. miR-501 upregulation and CYLD downregulation were associated with the development and progression of cervical cancer. miR-501 might be a potential therapeutic target for cervical cancer.

2. Materials and methods

2.1. Cell culture

Human cervical cancer cell line HeLa (ATCC, USA) was cultured in DMEM supplemented with penicillin/streptomycin and 10% fetal bovine serum (Omega, China), and incubated in a humidified incubator at 37 °C with 5% CO_2.

2.2. Human cervical cancer specimens

Forty-nine formalin-fixed human cervical carcinoma tissue samples were collected from the Department of Pathology, Dalian Municipal Central Hospital, Dalian, China, and embedded in paraffin for real-time qRT-PCR and immunohistochemistry analysis. The relevant guidelines and experimental protocols regarding the use of human samples for clinical and experimental research were approved by the Medical Ethics Committee of the Dalian Municipal Central Hospital. The clinical and pathological diagnoses as well as malignancy classifications were determined by pathologists, based on the FIGO classification system. Cervical cancer specimens were earlier examined histologically by hematoxylin and eosin (H&E) staining. Paired adjacent normal cervical tissues from the patients under study were obtained and used as negative control.

2.3. Cell transfection

At 24 h prior to transfection, HeLa cells were plated into 6-well plates at a density of 5×10^5 cells per well and were then transfected with 100 nM of miR-501 mimic (miR-501) or nonspecific sequence control (NC) using Lipofectamine 2000 (Invitrogen, USA) according to the manufacturer's protocol. siRNA against CYLD (siCYLD, GeneChem, China) transfection was achieved in a similar manner. The non-transfected HeLa cells (Control) was also a negative control. The transfected cells were prepared for RNA and protein extraction at 24 h and 48 h after transfection, respectively.

Knock-down of endogenous miR-501 was obtained through transfection with miR-501 inhibitor (501i) at a final concentration of 100 nM by Lipofectamine 2000 (Invitrogen, USA) in six-well plates (5×10^5 cells/well). The scrambled miRNA inhibitor (NCi), un-manipulated HeLa cells (Control), and co-transfections of miR-501 inhibitor and siCYLD (501i + siCYLD) were the negative controls. The transfected cells were harvested for RNA and protein extraction at 24 h and 72 h after transfection, respectively.

2.4. RNA extraction and real-time qRT-PCR

Total RNA was extracted from the parental and transfected HeLa cells respectively using Trizol (TransGen Biotech, China) reagent in accordance with the manufacturer's protocol. For the cervical cancer tissues, prior to RNA extraction, totally 5 sections of formalin-fixed and paraffin-embedded (FFPE) tissues (8–10 μm each) were deparaffinized with 100% xylene and 100% alcohol, digested by digestion buffer and protease (Invitrogen, USA), and incubated in an incubator at 55 °C for 1 h. Then total RNA was isolated using Trizol reagent according to the manufacturer's instructions.

For the real-time qRT-PCR analysis of miRNA, cDNA was synthesized using the TaqMan microRNA Reverse Transcription Kit (Life Technologies, USA). Quantitative PCR was carried out with MX3000P machine (Agilent Technologies, USA). PCR was carried out under the following conditions: 45 cycles of denaturation for 30 s at 95 °C, annealing for 30 s at 55 °C, and extension for 30 s at 72 °C. The miR-501 and endogenous control RNU6B primers were purchased from Ambion (Austin, USA). The expression value of miR-501 was normalized to RNU6B and was calculated using the $2^{(-\Delta\Delta CT)}$ formula.

For the real-time qRT-PCR analysis of mRNA, the reverse

transcription of purified RNA from the samples was performed using TransScript RT II one step gDNA Removel Reagent Kit (TransGen Biotech, China). The amplification for mRNA was carried out using 2 × TransStar Top Green pPCR SuperMix (TransGen Biotech, China) on an Agilent MX3000P instrument. The quantification of gene transcript was normalized to GAPDH and was calculated using the $2^{(-\Delta\Delta CT)}$ formula. All the real-time qRT-PCR experiments were done in triplicate. The sequences of primer pairs for CYLD and GAPDH were listed in the Supplementary Table 1.

2.5. Western blotting

Cells were harvested and washed twice with ice-cold PBS. Total proteins were extracted and then quantified by the BSA method using Bradford spectrometer (Sigma-Aldrich, USA). Same amounts of proteins prepared into equal volumes were loaded onto a gel (SDS-PAGE) and separated by electrophoresis. Using pre-stained protein molecular weight ladder as a guide, portions of the gel corresponding to the molecular weights of CYLD and β-tubulin proteins were sectioned out and transblotted onto a PVDF membrane (Millipore, USA). The membrane was blocked in 5% non-fat milk for one hour and then probed with polyclonal anti-rabbit CYLD antibody (1:1000, Proteintech, China), polyclonal anti-rabbit BCL-2 (1:400, Boster, China), polyclonal anti-rabbit BAX (1:400, Proteintech, China), polyclonal anti-rabbit NF-κB p65 (1:400, Boster, China), polyclonal anti-rabbit p-p65 (1:500, Abcam, China), and monoclonal anti-rabbit β-tubulin (1:500, Abgent, USA) primary antibodies overnight at 4 °C. After washing the membrane, HRP-conjugated rabbit anti-IgG secondary antibody (LI-COR Biosciences, USA) was applied to the above-mentioned proteins for 1 h and the bright bands were captured by Li-Cor Odyssey Infrared Imaging System (Version 3.0 software, LI-COR Biosciences, USA).

2.6. CCK-8 assay

The effects of miR-501 on HeLa cell proliferation was measured using CCK-8 cell proliferation kit (Sigma-Aldrich, USA). Twenty-four hours after transfection, triplicates of 3×10^3 cells per well were seeded in 96 well plates and cell proliferation was measured at 0 h, 24 h, 48 h and 72 h. The absorbance at 450 nm was measured at 2 h after adding 10 μl of CCK-8 reagent using Multiskan Go spectrometer (Thermo Fisher, USA).

2.7. Colony formation assay

To further assess the growth potential of the various group of cells mentioned above, colony formation assay was performed. Five hundred cells per well in triplicate were seeded in 6-well plates containing complete medium (DMEM with 10% FBS) and incubated for 7 days. The colonies were then fixed in 4% formalin, stained with 1% crystal violet for 20 min and then counted. This experiment was repeated 3 times to ensure reproducibility of the results.

2.8. Scratch wound healing assay

Scratch wound healing assay was performed to further interrogate the effects of miR-501 on migratory ability of cervical cancer cells. HeLa cells (2×10^5/well) were seeded into 6-well plates and transfected with miRNAs, miRNA inhibitors or siRNA respectively as mentioned as above. At 80% confluence of growth, the wounds were created with the aid of 200-μl pipette tip at the middle of each well and the debris was washed off with PBS. Cells were cultured in the serum-free medium for 24 h, 48 h, and 72 h. The wound closures were observed at the various aforementioned time points and the pictures of representative scrape lines were taken. Duplicate wells for each condition were examined, and each experiment was repeated for three consecutive times.

2.9. Transwell migration and invasion assays

Cells at a density of 1×10^5 cells per well in triplicate were plated in the upper chamber of the 24 well plate (pore size 8 μm, Corning, USA) containing 200 μl of serum-free DMEM medium. For invasion assay the base of the upper chambers was coated with extracellular matrigel (BD Biosciences, USA) to serve as artificial membrane. The lower chambers were filled with 700 μl complete medium to serve as a chemoattractant. The plates were incubated for 16 h at 5% CO_2 at 37 °C in a humidified incubator. Cells were fixed in methanol for 10 min, stained with 1% crystal violet for 20 min, and upper inserts were swabbed with dry cotton and dried for 30 min. The cells penetrating through the inserts were assessed by randomly choosing 5 fields under the microscope (Olympus IX73; Olympus Corporation, Japan).

2.10. Annexin V/Propidium iodide apoptosis assay

In order to assess the influences of miR-501 on the survival of cervical cancer cells, Annexin V/Propedium iodide (PI) apoptosis assay (BD Biosciences, USA) using flow cytometry was employed. In summary, duplicate of 5×10^5 cells/well of HeLa cells (Control), negative Control (NC), miR-501 mimic (miR-501), siCLYD, miR-501 inhibitor (501i) and co-transfections of miR-501 inhibitor and siCLYD (501i + siCYLD) were plated in 6-well plates containing DMEM with 10% FBS. After 24 h of incubation, cells were detached with trypsin, washed twice with ice-cold PBS and concurrently stained with 5 μl of Annexin V-FITC and 5 μl of propidium iodide (50 μg/ml) (KenGen, China) for 15 min at room temperature in the dark. The population of Annexin V-positive cells was evaluated by FACS Calibur flow cytometry (BD Biosciences, USA).

2.11. Immunohistochemistry

The expression of CYLD protein in cervical cancer specimens was analyzed by immunohistochemistry. Five micrometers blocky paraffin sections of cervical cancer and adjacent normal tissues were cut and mounted on poly-L-lysine-coated slides (Tianjin Fuyu Fine Chemical Co. Ltd, Tianjin, China). Subsequently, sections were deparaffinized, rehydrated and treated with citric acid buffer (pH 6.0) at 95–100 °C, 10 min for antigen retrieval. Endogenous peroxidase activity was blocked by incubation in 3% H_2O_2 for 20 min. Tissues were then incubated with primary polyclonal anti-rabbit CYLD antibody (1:100; proteintech, China) in a humidified chamber overnight at 4 °C. The following day the slides were washed with PBS and incubated with secondary antibody (Santa Cruz Biotechnology, USA) for 30 min. After washing, detection was determined by a Non-Biotin Horseradish Peroxidase Detection System and DAB substrate (Dako, USA). The sections were counterstained by hematoxylin (Tianjin Fuyu Fine Chemical Co. Ltd, Tianjin, China) and mounted in DPX (Tianjin Fuyu Fine Chemical Co. Ltd, Tianjin, China).

Immunohistochemistry results of CYLD expression in cervical tissues were observed and evaluated by 2 pathologists independently. CYLD protein was located on the cytoplasm of cervical squamous cancer cells and normal stratified squamous epithelial cells. The expression of CYLD was evaluated using a semi-quantitative immunohistochemical score (0–12 points) depending on the intensity (0–3 points) and proportion (0–4 points) [39]. The staining intensity was classified as following: 0 = negative staining, 1 = weak staining, 2 = moderate staining and 3 = strong staining. The proportion of positive staining was scored as following: no staining was 0, < 25% was 1, 25–50% was 2, 51–75% was 3 and > 75% was 4. The staining scores were calculated by multiplying the intensity score by the extent of positive cells staining, which yielded a range from 0 to 12 points. The cutoff number of positive CYLD expression was set as > 2.

2.12. Statistical analysis

SPSS version 15.0 and Graph Pad Prism version 5 (Graph Pad Software. Inc., USA) were used for the data analysis. Two matched clinical sample groups were analyzed by paired *t*-test and two unpaired groups were analyzed by unpaired *t*-test. One-way ANOVA followed by a Bonferroni-Dunn test was used to compare more than two groups. Chi-square test was used to assess the associations among the positive staining of CYLD and clinicopathological indices. The data were presented as mean ± SD and statistical significance was set at $P < 0.05$.

3. Results

3.1. miR-501 expression is increased and positively correlated with some clinicopathologic features of cervical cancer

To determine the clinical significance of miR-501 in the cervical cancer development and progression, we detected the expression of miR-501 in 49 paired of cervical cancer specimens and the corresponding normal cervical tissues. The real-time qRT-PCR results showed a significant increase in the expression of miR-501 in tumor tissues compared with normal tissues ($P = 0.021$, Fig. 1A and B). Furthermore, the relationship between miR-501 and the clinicopathologic characteristics of cervical cancer cases was studied and showed in Table 1. Each case was subdivided into a low-expression group and a high-expression group using the median value (2.31) of miR-501 as the cutoff number. Our results demonstrated that miR-501 expression was positively correlated with poor tumor differentiation ($P = 0.043$), tumor size ($P = 0.026$), FIGO stage ($P = 0.019$) and lymph node metastasis ($P = 0.010$). No significant correlation between miR-501 expression and age and HPV infection was observed ($P > 0.05$). These data indicate that miR-501 is associated with the development and progression of cervical cancer.

Table 1
Relationship between miR-501 expression and clinicopathologic characteristics in cervical cancer.

Characteristics	No. of cases	miR-501 expression		*P* value
		<2.31	≥2.31	
Age (year)				0.517
>50	22	9	13	
≤50	27	12	15	
Tumor size (cm)				0.026*
>4	31	13	18	
≤4	18	15	3	
FIGO stage				0.019*
I	30	17	13	
II	19	4	15	
HPV infection				0.072
Yes	21	12	9	
No	28	9	19	
Lymph node metastasis				0.010*
Yes	17	2	15	
No	32	19	13	
Differentiation				0.043*
Well	14	8	6	
Moderate	11	7	4	
Poor	24	6	18	

*$P < 0.05$.

3.2. CYLD is downregulated by miR-501 in cervical cancer cells

In a previous study, luciferase reporter assay results demonstrated that CYLD mRNA-3′UTR is directly targeted by miR-501 in HCC [22]. The predominant binding sites between miR-501 and the 3′-UTR of CYLD mRNA were shown in Fig. 2A. To confirm the expression of CYLD is regulated by miR-501 in cervical cancer, we transfected miR-501 mimic into HeLa cells. The real-time qRT-PCR analysis showed that miR-501 was dramatically upregulated compared to Control and NC groups (Supplementary Fig. 1A, $P < 0.001$), indicating that miR-501 is successfully transfected. CYLD was significantly reduced by miR-501 both at mRNA and protein levels shown by real-time qRT-PCR and Western blotting analyses, while similar results were observed in the siCYLD group (Fig. 2B and C, $P < 0.01$). There was no significant difference between Control and NC groups (Fig. 2B and C, $P > 0.05$).

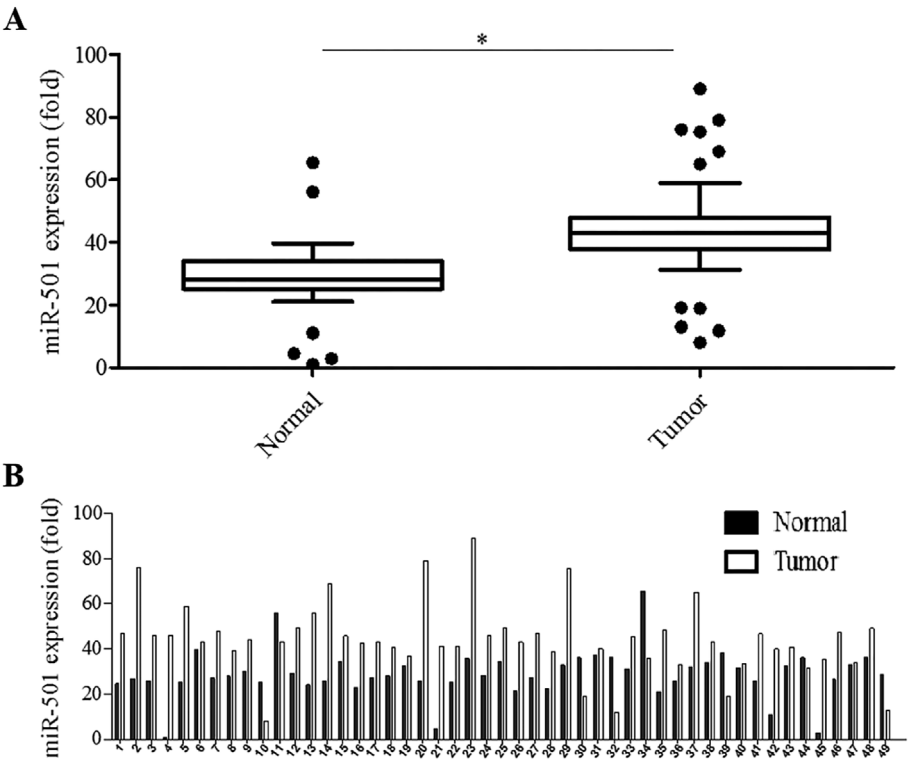

Fig. 1. miR-501 is overexpressed in cervical squamous cancer specimens. (A) RNA was extracted from the FFPE cervical cancer samples (Tumor, n = 49) and miR-501 were measured by real-time qRT-PCR. The paired adjacent normal cervical tissue (Normal, n = 49) was the negative control. Data were expressed as mean ± SD, *$P < 0.05$. (B) The relative quantification of miR-501 in each individual paired sample was shown.

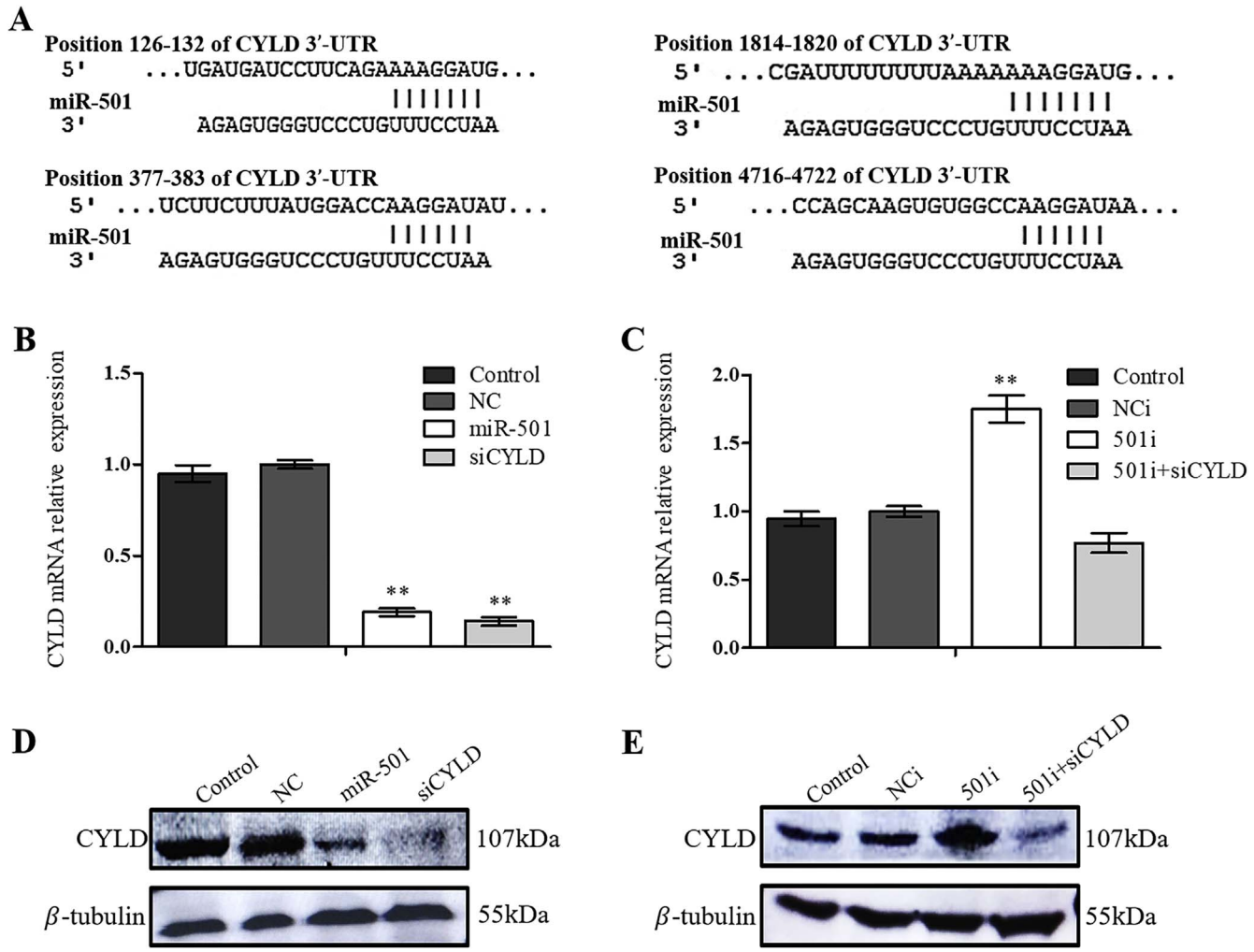

Fig. 2. miR-501 inhibits CYLD expression in cervical cancer cells. (A) The 3′-UTR of CYLD mRNA contains the putative binding sites of miR-501. (B) HeLa cells were transfected with miR-501 mimic (miR-501) using Lipofectamine 2000. Nonspecific sequence miRNA (NC) and non-transfected HeLa cells (Control) were the negative control. The siRNA against CYLD (siCYLD) was the positive control. The relative expression of CYLD mRNA was examined by real-time qRT-PCR after normalizing to GAPDH (n = 3), $^{**}P < 0.01$. (C) The expression of CYLD protein was determined by Western blotting after transfection described as in (B). β-tubulin was used as a loading control. The Western blotting results were analyzed by Odyssey infrared imaging software. (D) HeLa cells were transfected with miR-501 inhibitor (501i) using Lipofectamine 2000. Non-transfected HeLa cells (Control), scrambled miRNA inhibitor (NCi) and co-transfection of miR-501 inhibitor and siRNA against CYLD (501i + siCYLD) were the negative control. The relative expression of CYLD mRNA was measured by real-time qRT-PCR after normalizing to GAPDH (n = 3), $^{**}P < 0.01$. (E) The expression of CYLD protein was detected by Western blotting after transfection described as in (D). β-tubulin was used as a loading control and the Western blotting results were analyzed by Odyssey infrared imaging software.

These results indicate that CYLD is downregulated by miR-501 at post-transcriptional level in the cervical cancer cells.

Except the gain-of-function analysis, we also used loss-of-function experiments to confirm the regulatory relationship between miR-501 and CYLD. The miR-501 expression was blocked by the inhibitor as shown in Supplementary Fig. 1B ($P < 0.01$). Knockdown of miR-501 resulted in significant upregulation of CYLD both at mRNA and protein levels (Fig. 2D and E, $P < 0.01$). The expressions of CYLD in the Control, NCi and 501i + siCYLD groups were comparable (Fig. 2D and E, $P > 0.05$). These data further verify the negative regulatory between miR-501 and CYLD.

3.3. miR-501 promotes cell proliferative potential of cervical cancer via downregulating CYLD

To determine the influences of miR-501 on the cervical cancer, we first examined the cell proliferative capacity by CCK-8 and colony formation assays. As Fig. 3A and B shown, there was an overwhelming increase in both cell proliferation and average colony count in the miR-501 and siCYLD groups compared with the Control and NC groups ($P < 0.01$). No significant difference was observed when the Control group was compared with the NC group (Fig. 3A and B, $P > 0.05$). Similar results were noticed after comparing the miR-501 group with the siCYLD group (Fig. 3A and B, $P > 0.05$).

On the contrary, significant decrease in cell proliferation and average colony count was observed in the 501i group compared with the Control, NC and 501i + siCYLD groups (Fig. 3C and D, $P < 0.01$), while the results were comparable in the Control, NC and 501i + siCYLD groups (Fig. 3C and D, $P > 0.05$). In summary, the viability experiments reveal that miR-501 enhances the cervical cancer cell growth possibly through targeting CYLD.

3.4. miR-501 promotes the migratory and invasive abilities of cervical cancer cells through downregulating CYLD

Next, we aimed to interrogate whether miR-501 influences cervical cancer cell migratory and invasive capacities using scratch wound healing and Corning transwell assays. Scratch wound healing experiment determined the extent of cell migration by inferring to closure or narrowing of wound area in culturing cells at time points of 24 h, 48 h and 72 h respectively. Our results showed a significant decrease in wound area of miR-501 and siCYLD compared to Control and NC,

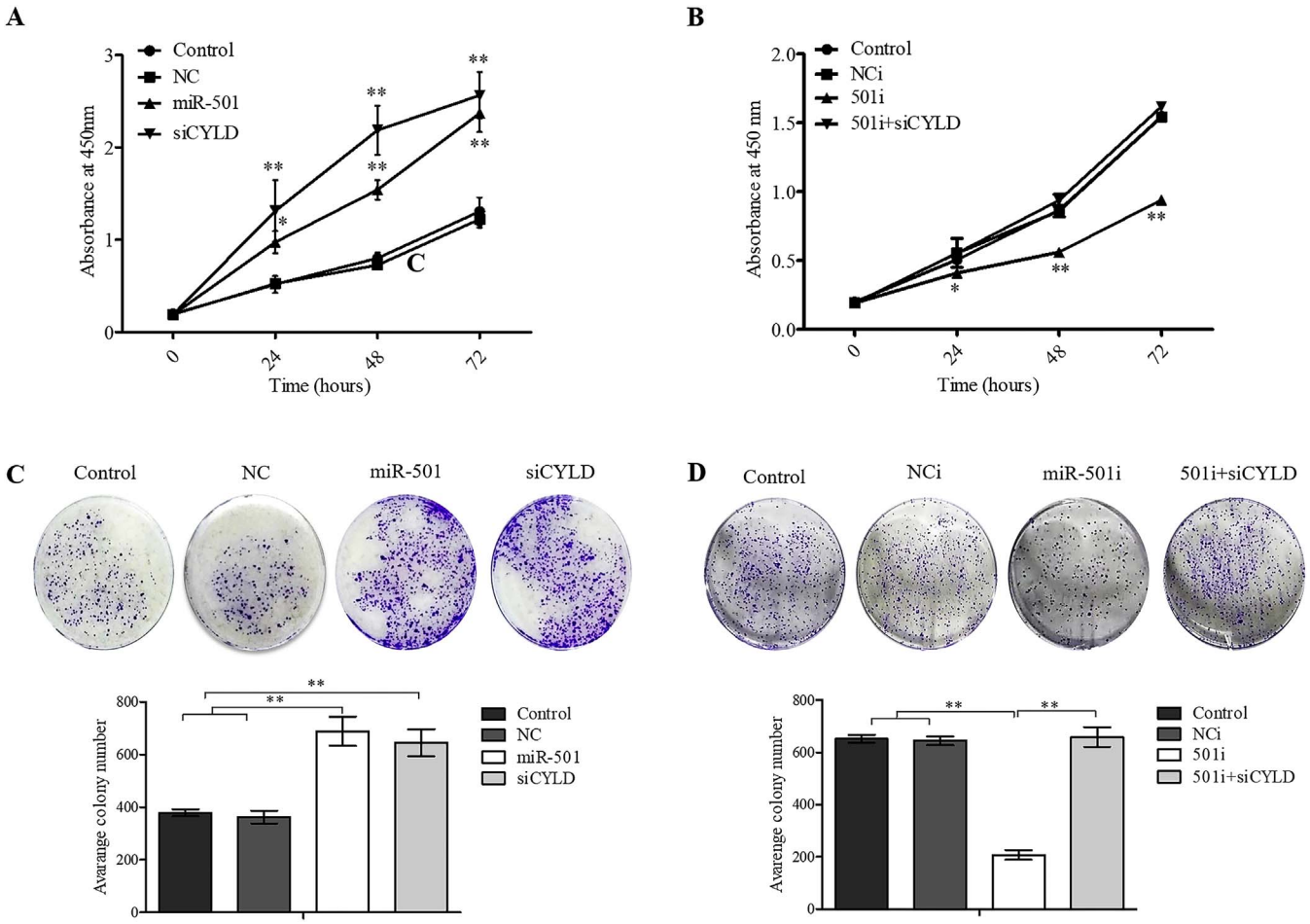

Fig. 3. miR-501 promotes the proliferation of cervical cancer cells. (A) HeLa cells were transfected with miRNA mimics or siRNA described as above and then replated in 96-well plates. The cell proliferative capacity was detected by the CCK-8 assay (n = 3), $*P < 0.05$, $**P < 0.01$. (B) HeLa cells transfected with miRNA mimics or siRNA were seeded in the 6-well plates and incubated for 1 week. The cell colonies were fixed, stained and counted (n = 3), $**P < 0.01$. (C) and (D) HeLa cells were transfected with miRNA inhibitors described as above, and the cell proliferative potential was determined by CCK-8 assay and cell colony formation assay (n = 3), $*P < 0.05$, $**P < 0.01$.

following 48 h and 72 h of incubation (Fig. 4A, $P < 0.01$). No significant difference in wound area was seen between Control and NC as well as between miR-501 and siCYLD (Fig. 4A, $P > 0.05$). Conversely, the wound area was larger in the 501i group compared to the Control, NCi and 501i + siCYLD groups after 24 h (Fig. 4B, $P < 0.05$), 48 h and 72 h of incubation (Fig. 4B, $P < 0.01$). When the Control, NCi and 501i + siCYLD groups were compared, no significant difference in wound closure was observed (Fig. 4B, $P > 0.05$).

Subsequently, we assessed the impacts of miR-501 on cervical cancer cell migration and invasion using Corning transwell assays. Our data showed that overexpression of miR-501 and silenced CYLD enhanced HeLa cells migration and invasion significantly compared to Control and NC (Fig. 4C and D, $P < 0.01$). No significant difference was observed between Control and NC and also, that of miR-501 and siCYLD (Fig. 4C and D, $P > 0.05$). On the contrary, migration and invasion was remarkably inhibited in 501i group compared to Control, NCi and 501i + siCYLD groups (Fig. 4E and F, $P < 0.01$), while the cell numbers penetrating through the inserts in the Control, NCi and 501i + siCYLD groups were comparable (Fig. 4E and F, $P > 0.05$). These results indicate that miR-501 enhances the cervical cancer cell migratory and invasive capacities via downregulating CYLD.

3.5. miR-501 inhibits the apoptosis of HeLa cells by downregulating CYLD

In order to reveal the underlying mechanism by which miR-501/CYLD axis works on cervical cancer cell proliferation, migration and invasion, we tested the apoptotic rate using flow cytometry. As Fig. 5A shown, the significant decrease in early, late and total apoptosis was observed after upregulation of miR-501 and knockdown of CYLD ($P < 0.05$), especially in early apoptosis. No significant deference was observed between Control and NC as well as miR-501 and siCYLD (Fig. 5A, $P > 0.05$). However, a substantial decrease in cell survival determined by Annexin V/PI experiment was observed in 501i as compared to Control, NCi and 501i + siCYLD (Fig. 5B, $P > < 0.01$). The significant decrease was seen in the early stage of apoptosis and total apoptosis ($P < 0.01$). No significant difference was observed when the Control, NCi, and 501i + siCYLD were compared with each other (Fig. 5B, $P > 0.05$). The expressions of pro- and anti-apoptotic genes, BCL-2 and BAX, were also examined by Western blotting. As Fig. 5C shown, BCL-2 protein was increased while BAX protein was decreased after miR-501 transfection. These data indicate that miR-501 is able to inhibit the apoptosis of cervical cancer cells likely via downregulating CYLD.

We then determined whether constitutive activation of NF-κB p65 is involved in the function of miR-501. Our results showed that NF-κB p65 and phosphorylated p65 (p-p65) proteins in the groups of miR-501 and siCYLD were significantly elevated compared with Control and NC groups (Fig. 5C, $P < 0.05$), suggesting that miR-501/CYLD axis might stimulate NF-κB p65 activation, therefore suppress the apoptosis and promote the cervical cancer cell proliferative, migratory and invasive potentials.

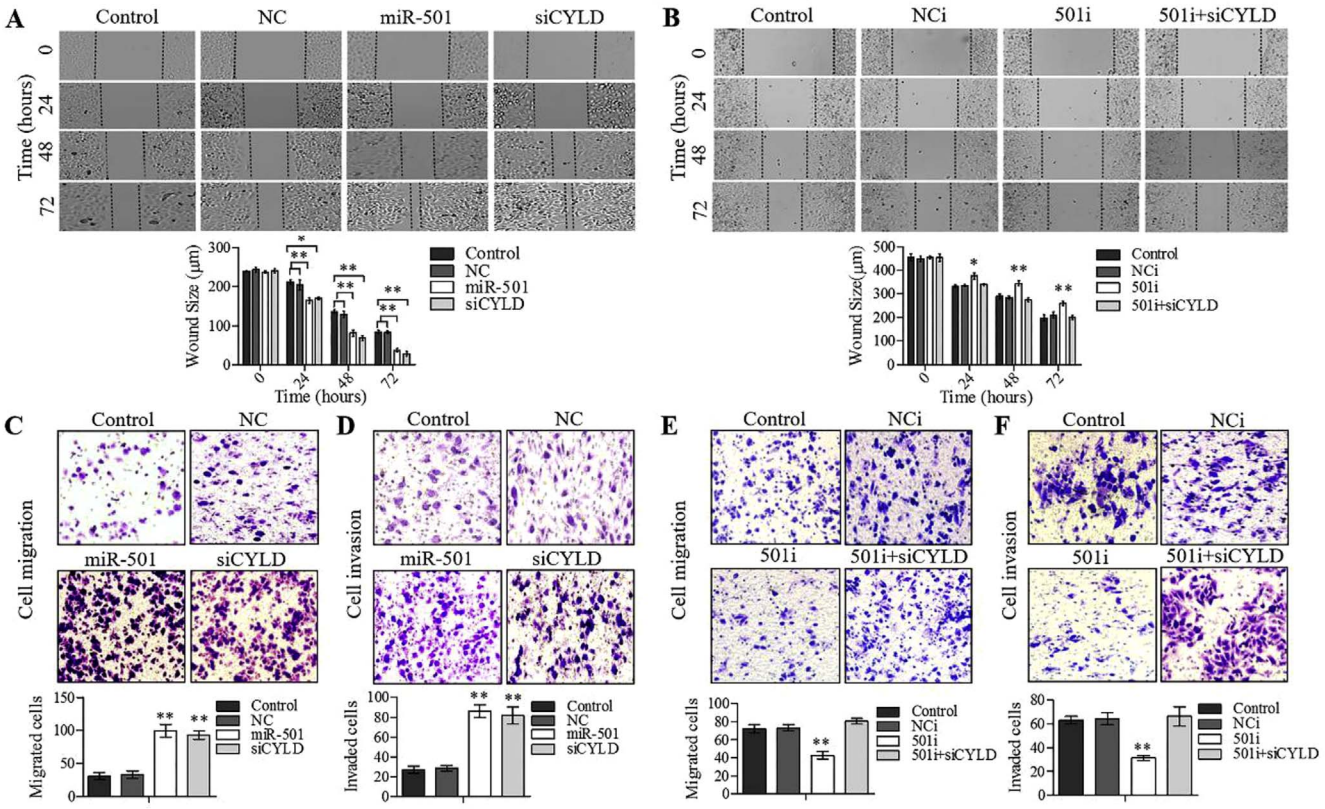

Fig. 4. miR-501 enhances the capacities of migration and invasion in cervical cancer cells. (A, C and D) HeLa cells were transfected with miRNA mimics or siRNA. Cell migratory and invasive potentials were determined by scratch wound healing assay and transwell chamber assays with or without matrigel (n = 3), $^{**}P < 0.01$. (B, E and F) The migratory and invasive potentials in the miR-501 knockdown HeLa cells were evaluated by scratch wound healing assay and transwell assays with or without matrigel (n = 3), $^{**}P < 0.01$. The representative pictures were shown. The wound size and cell numbers passing through the filter were indicated as mean ± SD respectively.

3.6. CYLD expression is downregulated in the cervical cancer tissues and negatively correlated with some clinicopathologic characteristics in cervical cancer

To assess the clinical significance of CYLD protein in cervical cancer, we investigated the expression of CYLD in 49 paired specimens (normal and cervical carcinoma) using immunohistochemical staining method. We found that CYLD was mainly expressed in the cytoplasm (Fig. 6A). The immunohistochemical score of CYLD in the cervical normal tissue was dramatically higher than that in the cervical cancer tissue (Fig. 6B, $P < 0.01$). Meanwhile, the positive percentage of CYLD showed similar trend in this cohort (Table 2, $P < 0.05$). Also, the relationship between CYLD expression and the clinicopathologic parameters of cervical cancer was studied. Each case was subdivided into CYLD positive group (+) and negative group (−) based on the cutoff number of immunohistochemical staining. As Table 3 shown, CYLD expression was negatively correlated with the tumor size ($P = 0.041$), FIGO stage ($P = 0.037$), lymph node metastasis ($P = 0.016$) and tumor differentiation ($P = 0.020$). No correlation was observed between CYLD expression and age and HPV infection ($P = 0.380$ and $P = 0.292$ respectively). These data demonstrate that CYLD plays a role on inhibiting the development and progression of cervical cancer.

4. Discussion

Although some advances have been made over the past decade, cervical cancer is still a public health concern especially in lower socioeconomic areas [40]. In this study, we investigated the oncogenic role of miR-501 in cervical cancer and disclosed the underlying mechanism based on the results from cervical cancer cell line and clinical specimens.

We firstly measured the level of miR-501 in cervical cancer samples using real-time qRT-PCR and found a dramatic increase of miR-501 in cervical cancer tissues than in adjacent normal tissues (Fig. 1). Additionally, miR-501 upregulation was significantly correlated with poor differentiation, tumor size, FIGO stage and lymph node metastasis (Table 1), suggesting that miR-501 functions as a tumor promoter in cervical cancer development and progression. We noticed that the research about the function of miR-501 in the oncology area is limited till now. In accordance with our results, miR-501 has been reported to be overexpressed in HCC, gastric cancer, conjunctival malignant melanoma in Denmark and retinoblastoma tissues [25,26]. Moreover, Fan et al. [24] found that miR-501 is a poor overall survival predictor in gastric cancer. Larsen et al. [25] reported that miR-501 expression level is associated with increased tumor thickness of Denmark conjunctival malignant melanoma. Taken together, the clinical evidence indicates that miR-501 is likely a critical promoter in the development, progression and metastasis of cervical cancer.

We then determined the functional role of miR-501 in the cervical cancer cells. Through the in vitro experiments and based on the gain-of- and loss-of-function analysis, we found that miR-501 promotes the potentials of cervical cancer cell proliferation, migration and invasion, whereas inhibits the cell apoptosis (Figs. 3–5). Huang et al. [22] reported that miR-501 enhances HCC cell proliferation via targeting CYLD and increased expression of cyclin D1 and c-myc. Fan et al. [24] demonstrated that miR-501 promotes gastric cancer stem cell like phenotype by directly targeting DKK1, NKD1 and GSK3β and activation of Wnt/β-catenin signaling. Our study confirmed CYLD is downregulated by miR-501 in the cervical cancer cell line (Fig. 2). We also observed that miR-501 is overexpressed, however, CYLD is downregulated, in the cervical cancer tissue compared to the normal cervical tissue (Fig. 6 and Table 2), further demonstrates the regulatory

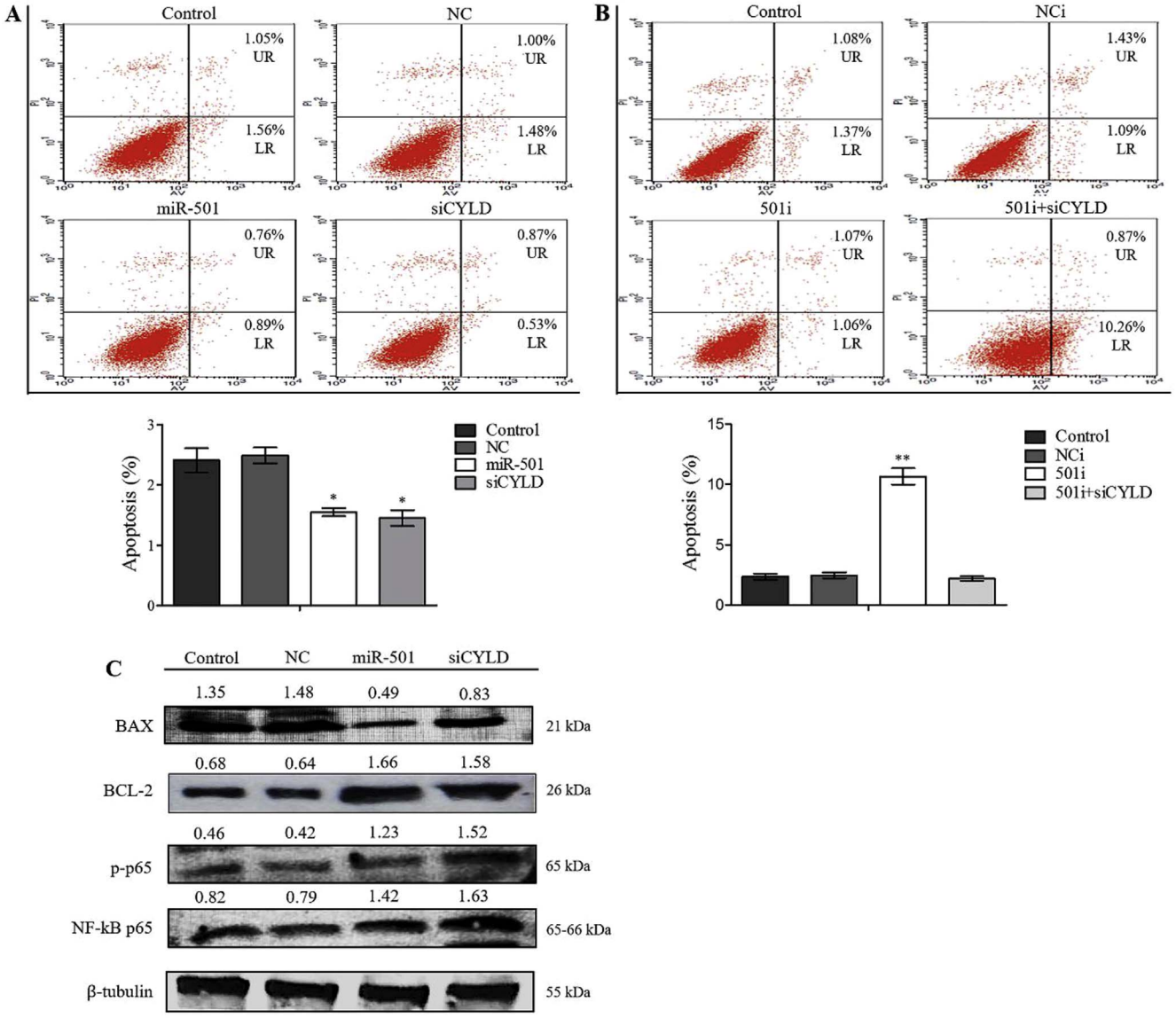

Fig. 5. miR-501 inhibits the apoptosis of HeLa cells. (A) The apoptotic rate was determined by Annexin V/PI assay following ectopic expression of miRNA mimics or siRNA (n = 3), $^{*}P < 0.05$. (B) The apoptotic rate was detected as described above in the HeLa cells following knockdown of miR-501 (n = 3), $^{*}P < 0.05$, $^{**}P < 0.01$. (C) NF-κB p65, phosphorylated p65 (p-p65), BCL-2 and BAX were analyzed using Western blotting. The relative quantities of these proteins were analyzed after normalization to β-tubulin.

relationship between miR-501 and CYLD. Moreover, the enhancement of cervical cancer cell proliferation, migration and invasion by miR-501 is likely due to the suppression of CYLD (Figs. 3 and 4).

CYLD is a known deubiquitinating enzyme that prevents the cleaving of NF-κB from its complex, thus negatively regulates NF-κB activation [41,42]. A previous study showed that CYLD deficiency can induce marked activation of NF-κB in germ cells and heightened expression of anti-apoptotic gene, BCL-2, resulting in the inhibition of apoptosis [41]. The blockade of NF-κB p65 promoted cell apoptosis via modulating BCL-2 and BAX expression has been reported in breast cancer [43]. In our current study, we found that miR-501 decreased the cervical cancer cell apoptotic rate, especially early apoptosis (Fig. 5). We then detected the commonest component of NF-κB, RelA (p65), phosphorylated p65, BCL-2 and BAX using Western blotting. Our results showed that NF-κB p65, phosphorylated p65 and BCL-2 expressions were all increased significantly by miR-501, whereas BAX was decreased (Fig. 5). These findings suggest that miR-501 inhibits cervical cancer cell apoptosis possibly through activation of NF-κB p65 and increased BCL-2 mediated by downregulating CYLD. Inhibition of cell apoptosis caused by miR-501 at least partially contributes to the enhanced cervical cancer proliferation.

Except apoptosis, NF-κB regulates transcription of DNA, cytokine production and cell survival as a protein complex [44,45]. Activation of NF-κB is critical for cancer development and progression [46]. Deng et al. [47] reported that overexpression of CYLD can augment anti-tumor activity by suppressing NF-κB survival signaling in human lung cancer cells. Our study demonstrated that miR-501 promotes the cervical cancer cell proliferation, migration and invasion likely through downregulating CYLD and subsequent activation of NF-κB p65. Except NF-κB signaling pathway, a recent in vitro study found that overexpression of CYLD inhibits SMAD7-mediated cell proliferation, migration and invasion in oral squamous cell carcinoma (OSCC) cells [48].

CYLD is referred to function as a tumor suppressor [49,50]. Our data showed that CYLD was highly expressed in the normal cervical tissue than cervical cancer tissue (Fig. 6, Table 2). In addition, CYLD downregulation was significantly correlated with tumor size, FIGO stage, lymph node metastasis and tumor differentiation (Table 3). In line with our results, CYLD has been reported to be downregulated in human HCC and colorectal cancer tissues compared with the surrounding non-malignant tissues, while it is correlated with metastasis [50,51].

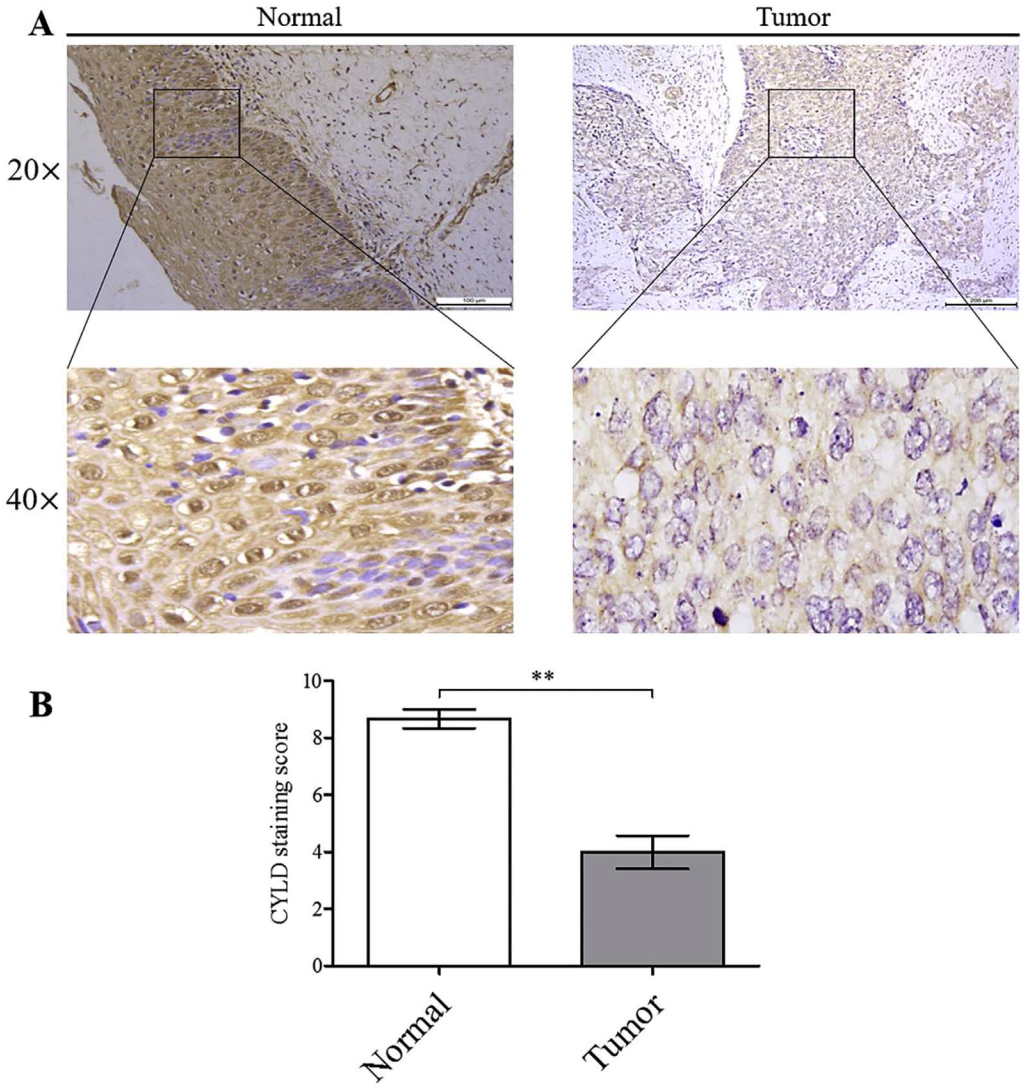

Fig. 6. CYLD protein is downregulated in the cervical cancer tissues. (A) CYLD protein was analyzed by immunohistochemistry in the normal cervical squamous epithelium (left) and cervical cancer tissue (right). Cells with brown granules in the cytoplasm were identified as CYLD positive. The magnification was × 20 and × 40 respectively. Scale bar = 100 μm. (B) The results of CYLD expression were evaluated by the staining scores. $^{**}P < 0.05$.

Table 2
Expression of CYLD protein in the normal cervical tissue and cervical cancer tissue.

	No. of cases	Positive (%)	Negative (%)	*P* value
Normal	49	41 (83.67%)	8 (16.33%)	$^{*}P < 0.05$
Tumor	49	17 (34.69%)	32 (65.31%)	

Normal group vs. tumor group ($^{*}P < 0.05$).

Moreover, Zhao et al. [52] reported a decrease tendency of CYLD expression from normal colorectal tissues, through benign adenomas to malignant colorectal cancer lesions. Thus, CYLD downregulation is possibly related to the development and progression of cervical cancer.

Persistent HPV infection is a widely recognized risk factor for cervical cancer. The link between miRNAs and HPV infection in the cervical cancer has been reported [53–55]. We also analyzed the role of miR-501 on the HPV infection. Our results showed that miR-501 was higher in the cervical cancer tissues with HPV infection, such as subtype 16, 18, 33, 35, and 52 (Table 1). But the difference did not reach the significance ($P = 0.072$), and this may due to the limited cases of our cohort. We will expand the cervical cancer samples and investigate further the relationship between miR-501 and HPV infection in the cervical cancer.

5. Conclusions

In summary, we experimentally prove that miR-501 enhances cervical cancer cell proliferation, migration and invasion upon downregulating CYLD and subsequent activation of NF-κB p65. miR-501 is overexpressed in the cervical cancer samples and is inversely correlated with the level of CYLD. miR-501 overexpression and CYLD downregulation contribute to the tumor size, FIGO stage, lymph node metastasis and tumor differentiation of cervical cancer. This suggests that miR-501 plays a key role in cervical cancer development and progression and therefore could be a potential therapeutic target for cervical cancer.

Ethical approval and consent to participate

The use of human tissue samples was in accordance with the relevant guidelines and regulations and the experimental protocols were approved by the Medical Ethics Committee of the Dalian Municipal Central Hospital. All patients provided written informed consent prior to participation in this study.

Table 3
Relationship between CYLD expression and clinicopathologic parameters in cervical cancer.

Characteristics	No. of cases	CYLD		*P* value
		(−)	(+)	
Age (year)				0.380
>50	22	10	12	
≤50	27	10	17	
Tumor size (cm)				0.041*
>4	31	16	15	
≤4	18	4	14	
FIGO stage				0.037*
I	30	14	16	
II	19	15	4	
HPV infection				0.292
Yes	21	11	10	
No	28	18	10	
Lymph node metastasis				0.016*
Yes	17	15	2	
No	32	14	18	
Differentiation				0.020*
Well	14	6	9	
Moderate	11	4	6	
Poor	24	19	5	

*$P < 0.05$.

Consent for publication

All authors read and approved the publication for this work.

Availability of data and material

The data are available from the corresponding author on reasonable request.

Competing interests

The authors declare that they have no conflicts of interest.

Funding

This work was supported by grants from the National Natural Science Foundation of China (No. 81172052 to Bo Song), from Natural Science Foundation of Liaoning Province (No. 201602235 to Bo Song), 'Yingcai' program of Dalian Medical University to Bo Song.

Authors' contributions

BS and JJZ designed the study. JS, YCX, IBY, ML, LMM and JS performed the experiments. JS, YCX, YL, XXX, LW, YD, and LH analyzed the data. LHL, JWT, JFJ revised the manuscript and assisted in study design. JS and BS wrote the manuscript. All the authors read and approved the final manuscript.

Acknowledgements

We would like to thank the Chinese Scholarship Council (CSC) for supporting Jaceline Gislaine Pires Sanches.

Appendix A. Supplementary data

Supplementary data related to this article can be found at http://dx.doi.org/10.1016/j.cbi.2018.02.024.

References

[1] A. Jemal, R. Siegel, J. Xu, E. Ward, Cancer statistics, 2010, CA Cancer J. Clin. 60 (2010) 277–300.
[2] J. Ferlay, H.R. Shin, F. Bray, D. Forman, C. Mathers, et al., Estimates of worldwide burden of cancer in 2008: GLOBOCAN 2008, Int. J. Cancer 127 (2010) 2893–2917.
[3] A. Jemal, F. Bray, M.M. Center, J. Ferlay, E. Ward, et al., Global cancer statistics, CA Cancer J. Clin. 61 (2011) 69–90.
[4] X. Liu, D. Wang, H. Liu, Y. Feng, T. Zhu, et al., Knockdown of astrocyte elevated gene-1 (AEG-1) in cervical cancer cells decreases their invasiveness, epithelial to mesenchymal transition, and chemoresistance, Cell Cycle 13 (2014) 1702–1707.
[5] C.J. Kim, J.K. Jeong, M. Park, T.S. Park, T.C. Park, et al., HPV oligonucleotide microarray-based detection of HPV genotypes in cervical neoplastic lesions, Gynecol. Oncol. 89 (2003) 210–217.
[6] S. Griffiths-Jones, R.J. Grocock, S. van Dongen, A. Bateman, A.J. Enright, miRBase: microRNA sequences, targets and gene nomenclature, Nucleic Acids Res. 34 (2006) 140–144.
[7] J.S. Mattick, I.V. Makunin, Small regulatory RNAs in mammals, Hum. Mol. Genet. 14 (2005) 121–132.
[8] E. Berezikov, R.H. Plasterk, Camels and zebrafish, viruses and cancer: a microRNA update, Hum. Mol. Genet. 14 (2005) 183–190.
[9] B. Bartel, MicroRNAs directing siRNA biogenesis, Nat. Struct. Mol. Biol. 12 (2005) 569–571.
[10] P.D. Zamore, B. Haley, Ribo-genome: the big world of small RNAs, Science 309 (2005) 1519–1524.
[11] C.M. Croce, G.A. Calin, miRNAs, cancer, and stem cell division, Cell 122 (2005) 6–7.
[12] K. Banno, M. Iida, M. Yanokura, I. Kisu, T. Iwata, et al., MicroRNA in cervical cancer: OncomiRs and tumor suppressor miRs in diagnosis and treatment, Sci. World J. 2014 (2014) 178075.
[13] K. Gocze, K. Gombos, K. Juhasz, K. Kovacs, B. Kajtar, et al., Unique MicroRNA expression profile in cervical cancer, Anticancer Res. 33 (2013) 2561–2568.
[14] J.M. Cummins, V.E. Velculescu, Implications of micro-RNA profiling for cancer diagnosis, Oncogene 25 (2006) 6220–6227.
[15] H. He, K. Jazdzewski, W. Li, S. Liyanarachchi, R. Nagy, et al., The role of microRNA genes in papillary thyroid carcinoma, Proc. Natl. Acad. Sci. U. S. A. 102 (2005) 19075–19080.
[16] M.V. Iorio, M. Ferracin, C.G. Liu, A. Veronese, R. Spizzo, et al., MicroRNA gene expression deregulation in human breast cancer, Cancer Res. 65 (2005) 7065–7070.
[17] M.Z. Michael, S.M. O' Connor, N.G. van Holst Pellekaan, G.P. Young, R.J. James, Reduced accumulation of specific microRNAs in colorectal neoplasia, Mol. Cancer Res. 1 (2003) 882–891.
[18] J. Takamizawa, H. Konishi, K. Yanagisawa, S. Tomida, H. Osada, et al., Reduced expression of the let-7 microRNAs in human lung cancers in association with shortened postoperative survival, Cancer Res. 64 (2004) 3753–3756.
[19] M. Osaki, F. Takeshita, T. Ochiya, MicroRNAs as biomarkers and therapeutic drugs in human cancer, Biomarkers 13 (2008) 658–670.
[20] C.P. Lin, L. He, Noncoding RNAs in cancer development, Annu. Rev. Cancer Biol. 1 (2017) 163–184.
[21] J. Jin, S. Tang, L. Xia, R. Du, H. Xie, et al., MicroRNA-501 promotes HBV replication by targeting HBXIP, Biochem. Biophys. Res. Commun. 430 (2013) 1228–1233.
[22] D.H. Huang, G.Y. Wang, J.W. Zhang, Y. Li, X.C. Zeng, et al., MiR-501-5p regulates CYLD expression and promotes cell proliferation in human hepatocellular carcinoma, Jpn. J. Clin. Oncol. 45 (2015) 738–744.
[23] C. Zhang, H. Du, Screening key miRNAs for human hepatocellular carcinoma based on miRNA-mRNA functional synergistic network, Neoplasma 64 (2017) 816–823.
[24] D. Fan, B. Ren, X. Yang, J. Liu, Z. Zhang, Upregulation of miR-501-5p activates the wnt/β-catenin signaling pathway and enhances stem cell-like phenotype in gastric cancer, J. Exp. Clin. Cancer Res. 35 (2016) 177.
[25] A.C. Larsen, Conjunctival malignant melanoma in Denmark. Epidemiology, treatment and prognosis with special emphasis on tumorigenesis and genetic profile, Acta Ophthalmol. 94 (2016) 842.
[26] N. Venkatesan, P.R. Deepa, V. Khetan, S. Krishnakumar, Computational and in vitro investigation of miRNA-Gene regulations in retinoblastoma pathogenesis: miRNA mimics strategy, Bioinform. Biol. Insights 9 (2015) 89–101.
[27] G.R. Bignell, W. Warren, S. Seal, M. Takahashi, E. Rapley, et al., Identification of the familial cylindromatosis tumour-suppressor gene, Nat. Genet. 25 (2000) 160–165.
[28] A. Kovalenko, C. Chable-Bessia, G. Cantarella, A. Israel, D. Wallach, et al., The tumour suppressor CYLD negatively regulates NF-kappaB signalling by deubiquitination, Nature 424 (2003) 801–805.
[29] S. Saggar, K.A. Chernoff, S. Lodha, L. Horev, S. Kohl, et al., CYLD mutations in familial skin appendage tumours, J. Med. Genet. 45 (2008) 298–302.
[30] C.M. Annunziata, R.E. Davis, Y. Demchenko, W. Bellamy, A. Gabrea, et al., Frequent engagement of the classical and alternative NF-kappaB pathways by diverse genetic abnormalities in multiple myeloma, Cancer Cell 12 (2007) 115–130.
[31] J.J. Keats, R. Fonseca, M. Chesi, R. Schop, A. Baker, et al., Promiscuous mutations activate the noncanonical NF-kappaB pathway in multiple myeloma, Cancer Cell 12 (2007) 131–144.
[32] P. Ströbel, A. Zettl, Z. Ren, P. Starostik, H. Riedmiller, et al., Spiradenocylindroma of the kidney: clinical and genetic findings suggesting a role of somatic mutation of the CYLD1 gene in the oncogenesis of an unusual renal neoplasm, Am. J. Surg. Pathol. 26 (2002) 119–124.
[33] K. Hashimoto, N. Mori, T. Tamesa, T. Okada, S. Kawauchi, et al., Analysis of DNA copy number aberrations in hepatitis C virus-associated hepatocellular carcinomas by conventional CGH and array CGH, Mod. Pathol. 17 (2004) 617–622.
[34] Y. Hirai, Y. Kawamata, N. Takeshima, R. Furuta, T. Kitagawa, et al., Conventional and array-based comparative genomic hybridization analyses of novel cell lines harboring HPV18 from glassy cell carcinoma of the uterine cervix, Int. J. Oncol. 24 (2004) 977–986.

[35] C. Hellerbrand, E. Bumes, F. Bataille, W. Dietmaier, R. Massoumi, et al., Reduced expression of CYLD in human colon and hepatocellular carcinomas, Carcinogenesis 28 (2007) 21–27.
[36] M. Hayashi, H. Jono, S. Shinriki, T. Nakamura, J. Guo, et al., Clinical significance of CYLD downregulation in breast cancer, Breast Cancer Res. Treat. 143 (2014) 447–457.
[37] L.L. Deng, Y.X. Shao, H.F. Lv, H.B. Deng, F.Z. Lv, Over-expressing CYLD augments antitumor activity of TRAIL by inhibiting the NF-κB survival signaling in lung cancer cells, Neoplasma 59 (2012) 18–29.
[38] E. Trompouki, E. Hatzivassiliou, T. Tsichritzis, H. Farmer, A. Ashworth, et al., CYLD is a deubiquitinating enzyme that negatively regulates NF-kappaB activation by TNFR family members, Nature 424 (2003) 793–796.
[39] L. Yu, Y. Lu, X. Han, W. Zhao, J. Li, et al., microRNA -140-5p inhibits colorectal cancer invasion and metastasis by targeting ADAMTS5 and IGFBP5, Stem Cell Res. Ther. 7 (2016) 180.
[40] A.W. LaVigne, S.A. Triedman, T.C. Randall, E.L. Trimble, A.N. Viswanathan, Cervical cancer in low and middle income countries: Addressing barriers to radiotherapy delivery, Gynecol. Oncol. Rep. 22 (2017) 16–20 Review.
[41] A. Wright, W.W. Reiley, M. Chang, W. Jin, A.J. Lee, et al., Regulation of early wave of germ cell apoptosis and spermatogenesis by deubiquitinating enzyme CYLD, Dev. Cell 13 (2007) 705–716.
[42] S.C. Sun, CYLD: a tumor suppressor deubiquitinase regulating NF-kappaB activation and diverse biological processes, Cell Death Differ. 17 (2010) 25–34.
[43] K. Velaei, N. Samadi, S. Soltani, B. Barazvan, J. Soleimani Rad, NF-κBP65 transcription factor modulates resistance to doxorubicin through ABC transporters in breast cancer, Breast Cancer 24 (2017) 552–561.
[44] M.S. Hayden, S. Ghosh, Shared principles in NF-kappaB signaling, Cell 132 (2008) 344–362.
[45] N.D. Perkins, Post-translational modifications regulating the activity and function of the nuclear factor kappa B pathway, Oncogene 25 (2006) 6717–6730.
[46] J. Inoue, J. Gohda, T. Akiyama, K. Semba, NF-kappaB activation in development and progression of cancer, Cancer Sci. 98 (2007) 268–274 Review.
[47] L.L. Deng, Y.X. Shao, H.B. Deng, F.Z. Lu, Overexpressing CYLD augments antitumor activity of TRAIL by inhibiting the NF-κB survival signaling in lung cancer cells, Neoplasma 59 (2012) 18–29.
[48] W.L. Ge, J.F. Xu, J. Hu, Regulation of oral squamous cell carcinoma proliferation through crosstalk between SMAD7 and CYLD, Cell Physiol. Biochem. 38 (2016) 1209–1217.
[49] P. Miliani de Marval, S. Lutfeali, J.Y. Jin, et al., CYLD inhibits tumorigenesis and metastasis by blocking JNK/AP1 signaling at multiple levels, Cancer Prev. Res. 4 (2011) 851–859.
[50] H. Kinoshita, H. Okabe, T. Beppu, A. Chikamoto, H. Hayashi, K. Imai, et al., CYLD downregulation is correlated with tumor development in patients with hepatocellular carcinoma, Mol. Clin. Oncol. 1 (2013) 309–314.
[51] F. Ni, H. Zhao, H. Cui, Z.W. Wu, L. Chen, et al., MicroRNA-362-5p promotes tumor growth and metastasis by targeting CYLD in hepatocellular carcinoma, Cancer Lett. 356 (2015) 809–818.
[52] H. Zhao, F. Xu, M. Jin, G. An, G. Feng, CYLD expression in benign, malignant and metastatic lesions of colorectal epithelium and its prognostic role in colorectal carcinoma, Int. J. Clin. Exp. Pathol. 9 (2016) 4909–4916.
[53] S.S. Shah, S. Senapati, F. Klacsmann, D.L. Miller, J.J. Johnson, et al., Current Technologies and recent developments for screening of HPV-associated cervical and oropharyngeal cancers, Cancers (Basel) 8 (2016) 85 Review.
[54] M. Lin, X.Y. Xue, S.Z. Liang, Y.X. Li, Y.Y. Lv, et al., MiR-187 overexpression inhibits cervical cancer progression by targeting HPV16 E6, Oncotarget 8 (2017) 62914–62926.
[55] J. Li, Q. Liu, L.H. Clark, H. Qiu, V.L. Bae-Jump, et al., Deregulated miRNAs in human cervical cancer: functional importance and potential clinical use, Future Oncol. 13 (2017) 743–753 Review.